

# A Glimpse into IEEE 802.11be Channels: Can They Improve CSI-based Sensing?

Marco Cominelli\*, Shabbir Raza<sup>†</sup>, Renato Lo Cigno<sup>†</sup>, Francesco Gringoli<sup>†</sup>

\*DEIB, Politecnico di Milano, Italy. marco.cominelli@polimi.it

<sup>†</sup>DII, University of Brescia and CNIT, Italy. {shabbir.raza, francesco.gringoli, renato.locigno}@unibs.it

**Abstract**—Wireless sensing based on Channel State Information (CSI) is rapidly spreading with the advent of 6G and newer Wi-Fi versions. Today, the CSI is regarded as one of the most promising elements for boosting service innovation on indoor device-free sensing. In addition, the wide adoption of the latest IEEE 802.11be standard, commonly known as Wi-Fi 7, might open up new possibilities for Wi-Fi sensing applications with even larger bandwidths, up to 320 MHz, and 4096 sub-carriers per spatial stream. However, researchers have still limited access to CSI extraction tools for such systems. In this work, we devise a framework based on software-defined radios to investigate the potential implications of the new Wi-Fi features, namely the wider channels and the higher number of sub-carriers, on a device-free positioning system based on position fingerprinting. In particular, we analyze the impact and the performance variations of this new technology across different bands in a position classification system, which has proven to be very accurate with previous versions of Wi-Fi. Our preliminary findings set some clear guidelines to direct future research efforts towards a better usage of newer Wi-Fi channels for sensing purposes. Furthermore, we publicly release our framework to the community of researchers and engineers for developing better Wi-Fi sensing solutions for smart homes, health care, and Internet-of-Things applications in general.

## I. MOTIVATION

Wi-Fi sensing based on CSI analysis is attracting increasing interest in light of 6G and future Wi-Fi versions, as it is deemed one of the promising technologies to enhance applications with contextual information [1]–[3]. Many scientific questions are still open, which we cannot discuss here in detail, but one raises our curiosity: How will emerging technologies influence sensing precision? This paper addresses this interesting question in the context of Wi-Fi, and in particular of the upcoming IEEE 802.11be standard [4], setting a solid ground and a clear path on how to dive appropriately into this interesting subject in future works. Current Wi-Fi communications are based on Orthogonal Frequency Division Multiplexing (OFDM), thus the bandwidth and the spacing of the OFDM subcarriers are critical parameters that affect the quality of the CSI, and hence the quality of *sensing*

operations. The central frequency is another parameter influencing the sensing performance (Wi-Fi can work at 2.4 GHz, 5.5 GHz, or above 6 GHz). However, in this work, we pick a fixed central frequency and focus on assessing the impact of the bandwidth rather than the wavelength. IEEE 802.11ax [5] and 802.11be [4] share the same sub-carrier spacing of 78.125 kHz for high-throughput frames, but 802.11be introduces the 320 MHz bandwidth and the Extremely High Throughput (EHT) mode at the PHY layer. Understanding its impact on sensing is very important.

Even though commercial devices supporting IEEE 802.11be are now approaching the market, researchers have limited options to work with CSI extraction tools that are compatible with the latest Wi-Fi standard. To our knowledge, the only solution today is to use Software Defined Radio (SDR) platforms, either running closed-source software like PicoScenes [6] or some custom implementation. CSI extractors that work also on commercial systems are limited to the IEEE 802.11ax standard (e.g., again PicoScenes for Intel network cards or AX-CSI [7] on Broadcom cards). Older CSI extractors are still popular today, with the Linux 802.11n CSI Tool [8] still being widely used today for Wi-Fi sensing studies [9], but they cannot be used to assess technology-related advances.

In this work, we adopt a custom SDR implementation based on Ettus devices and supported by Matlab. On the transmitter side the IQ samples corresponding to a transmission frame are prepared in Matlab and then passed to the Ettus device that implements the Digital to Analog Converter (DAC) and the transmission on-air; on the receiver side, the Ettus device implements the antenna front-end and the Analog-to-Digital Converter (ADC), and the Matlab script recovers the received frames from the received sampled radio signals. We detail this setup in Section II. In the rest of the paper we explore the impact of the Wi-Fi signals bandwidth on the performance of a target sensing application, specifically, a simple device-free localization algorithm described in Section III. Our results offer preliminary insights into the relation between the sensing techniques and the amount of information the signal collects from the environment during propagation.

This research was partially supported at University of Brescia through project MOST (Sustainable Mobility Center CN00000023) Spoke 7 "CCAM" (CUP E13C22000980001); project ISP5G+ (CUP D33C22001300002) part of the SERICS program (PE000000014); project EMBRACE (CUP E63C22002070006) part of the RESTART program (PE000000001), and at Politecnico di Milano within MICS (PE000000004), CUP D43C22003120001. All projects are under the NRRP MUR program funded by the EU-NGEU.

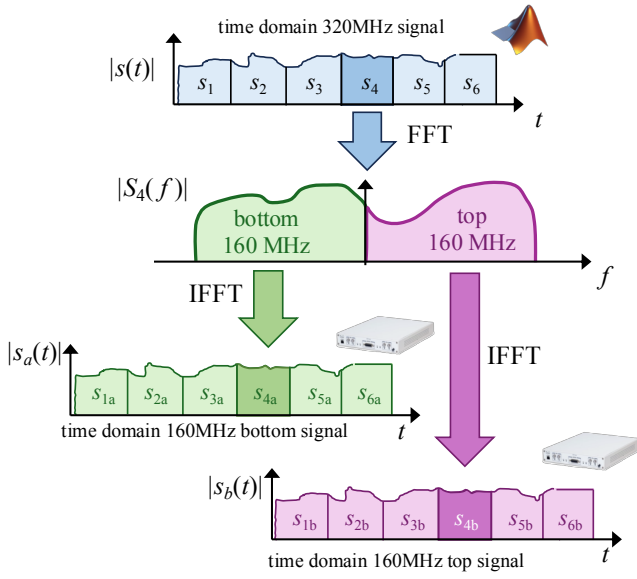


Figure 1: Illustration of the procedure used to split a 320-MHz signal generated by MATLAB into two halves (each of 160 MHz) that are compatible with the SDR front end. Each OFDM symbol from the original signal at 320 MHz is processed in the frequency domain to create the corresponding copies and generate the two signals carrying respectively the bottom and top part of the original spectrum. Here we emphasise the process for symbol  $s_4$ .

## II. EMULATING IEEE 802.11BE TRANSMISSIONS

The methodology proposed in this work uses two MATLAB instances to *i*) generate IQ samples corresponding to well-formed IEEE 802.11be frames at the transmitter and *ii*) extract and process the CSI from each frame at the receiver. The Wi-Fi frames are exchanged over the air using wideband SDR platforms. Specifically, we use two Ettus X310 SDRs motherboards (one for transmitting and one for receiving) each equipped with a pair of UBX 160 daughterboards. Even though the UBX 160 daughterboards have a maximum bandwidth of 160 MHz, we can successfully transmit and receive 320 MHz Wi-Fi frames by splitting the signals into two halves, each transmitted by a separate daughterboard. This process, shown in Fig. 1 and key to experiment with 320 MHz bandwidth, is now explained in detail.

### A. Transmitter Operations

On the transmitter, a sequence of IQ samples corresponding to a well-formed Wi-Fi frame is generated using the MATLAB WLAN toolbox. The result is a complex signal in the time domain sampled at 320 MSample/s. From the time-domain signal, the sequence of OFDM symbols is recovered by reversing the signal construction process of the EHT-PHY<sup>1</sup> specification ([4], Chapter 36). Specifically, the WLAN toolbox is first used to identify the OFDM symbols' boundaries; then the windowing and the Guard Interval (GI) are removed, and the Fast Fourier Transform (FFT) is applied to each

<sup>1</sup>EHT-PHY is the physical layer of IEEE 802.11be, which is named Extremely High Throughput (EHT).

OFDM symbol to obtain all its subcarrier coefficients, that is, its spectral content. In the case of 320-MHz 802.11be frames every OFDM symbol consists of 4096 subcarriers, equally spaced by 78.125 kHz. This processing step is illustrated in the first part in Fig. 1, where each OFDM symbol signal generated by MATLAB in the time domain is transformed into its corresponding representation in the frequency domain.

The 4096 OFDM subcarriers are split in two equal parts: top and bottom, each one with 2048 subcarriers. Then, each part is processed with the same operations in reverse order to obtain two signals in the time domain sampled at 160 MSample/s, corresponding to the top and the bottom halves of the original signal's spectrum. The top and bottom parts of the 320 MHz signal are sent to the two daughterboards mounted on the transmitter after an upsampling operation that matches the signal bandwidth to the rate of the master clock on the X310 SDR, which is 200 MHz. The two daughterboards are tuned at  $\pm 80$  MHz from the central frequency of the Wi-Fi channel and are connected to an RF multiplexer so that the resulting 320 MHz signal is transmitted from a single antenna as if a single device generated it.

It is important to note that the double-radio approach described so far splits the wideband signal over two carriers, thus introducing a double-hump shape in the signal's spectrum, with the two peaks centered around  $-80$  MHz and  $80$  MHz, that is, the central frequencies of the two daughterboards. To mitigate this effect, we apply a *pre-equalization* mask to the signals fed to the two transmit daughterboards. The specific shape of the pre-equalization masks is determined before the on-air experiments are run. Its actual design is derived empirically equalizing the spectral content of frames preambles transmitted over a coaxial cable so that it results flat on the entire 320 MHz channel.

### B. Receiver Operations

The operations at the receiver are the inverse of the ones performed at the transmitter. First, the 320 MHz radio signal is extracted from a single antenna and fed to a splitter that generates two identical copies without power loss. Thus, two copies of the same signal are fed to the two daughterboards on the receiving X310 SDR. The daughterboards are tuned at the same frequencies as their transmitter counterparts ( $\pm 80$  MHz from the central frequency) so that each of them only captures the upper and the lower portion of the spectrum of the original signal.

The daughterboards work at 200 MSample/s, so each of the portions of the spectrum must be properly and accurately filtered to retain exactly the 160 MHz top or bottom part of the spectrum respectively. Then they are up-sampled at 320 MSample/s and the two signals are shifted at the proper frequency and added together to get the original 320 MHz Wi-Fi frame. Finally, the MATLAB WLAN toolbox extracts the CSI.

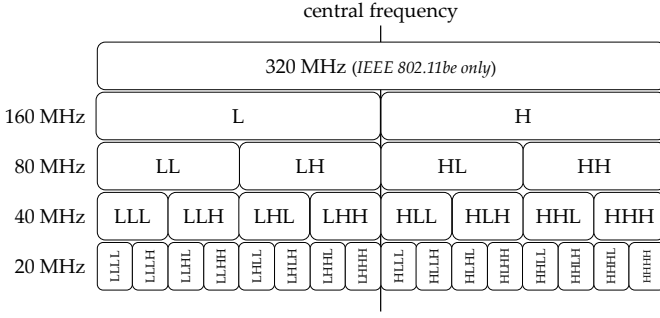


Figure 2: Visualization of the relation between standard Wi-Fi channels and naming scheme used in the experiments for each bandwidth.

### C. Other Considerations

Several other considerations are worth mentioning to properly appreciate the methodology adopted. First, the transmitting and receiving X310 SDRs must be synchronized using an Ettus Octoclock device that provides a Pulse Per Second (1 PPS) and 10 MHz reference signals. The synchronization between transmitter and receiver is fundamental in this setup for two reasons: *i)* the synchronization allows the receiver to capture samples only when the transmitter is active, effectively reducing the storage required for each experiment; *ii)* the synchronization makes the processing much faster because the receiver does not need to search for frame boundaries. To achieve this second goal, we developed software in C++ to control the synchronized transmission and reception of 320 MHz signals<sup>2</sup>. To the best of our knowledge, no other open-source code can collect and analyze 320-MHz Wi-Fi frames (PicoScenes supports 802.11be frames but is mostly closed-source).

Second, the X310 SDRs cannot work above 6 GHz, in the spectrum slab actually assigned to 802.11be. Hence, we must work on lower frequencies during our experiments. Given the central frequency of the 320 MHz Wi-Fi channel, we analyze all the possible sub-channels as shown in Fig. 2. This *segmentation* of the Wi-Fi channels can be used to examine the impact of the different bandwidths on the sensing performance and compare the sensing performance when using data from different sub-channels.

### III. SENSING ARCHITECTURE

Several CSI-based sensing architectures and methods have been considered by the research community over the last few years. Different frameworks are often tied to specific sensing applications. A detailed discussion about their merits and limitations is beyond the scope of this contribution; interested readers can explore more on this subject starting from the recent survey in [2]. Here, we focus on a device-free positioning framework using a fingerprinting approach [10] based on a Convolutional Neural Network (CNN), which has the merit of being simple and allowing easy parameter

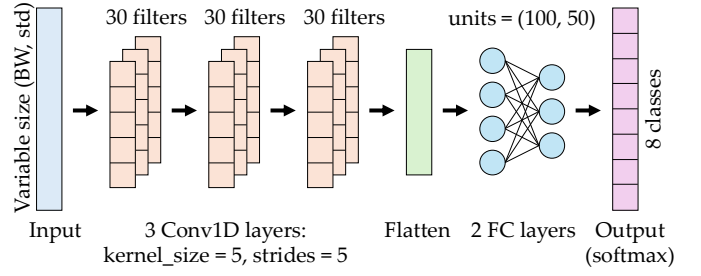


Figure 3: Architecture of the neural network for the positioning task. All the hidden layers use a ReLU activation function.

adjustment. We have successfully implemented and used the approach in other works [11], [12], thus we are reliant to isolate the appropriate insights due to bandwidth. Moreover, the focus of our work is not on the sensing algorithm, and we think that the impact of different bandwidths is similar on most algorithms, unless they are specifically tuned having in mind a particular bandwidth and signal structure.

Figure 3 shows the architecture of the CNN employed in this work. In short, the CNN is utilized to solve a classification problem where every input CSI is mapped onto one of eight target positions. The CNN has a straightforward structure, with three convolutional layers followed by a flattening layer and two fully-connected (FC) layers. The activation function in all the hidden layers is a Rectified Linear Unit (ReLU) function, while the output layer uses a Softmax activation function. The number and the shape of the hidden layers are fixed; the only variable in the definition of the CNN architecture is the size of the input layer, which depends on the bandwidth of the input CSI and on the Wi-Fi standard considered.

This work considers only Single-Input Single-Output (SISO) systems, allowing to focus only on the signal bandwidth as the primary variable of our analysis, leaving out the effects caused by multiple spatial streams and different antenna patterns that may influence the sensing performance.

### IV. EXPERIMENTS

The experimental work was carried out in the ANS<sup>3</sup> telecommunication laboratory. Figure 4 shows the layout of the experimental site, highlighting the location of the transmitter (TX) and receiver (RX), as well as the eight target positions on which we evaluate the performance of the device-free positioning system.

We perform a separate data collection for each of the bandwidths reported in Fig. 2 and for two different Wi-Fi standards, namely 802.11ac and 802.11be. In the analysis discussed in Section V, we also consider smaller bandwidths of 10 MHz only to discover any trend in the relation between the bandwidth and the sensing accuracy. During the data collection process, one person stands on each of the eight target positions while TX transmits 800 Wi-Fi frames at

<sup>2</sup>Code available at <https://github.com/ansresearch/sensing-80211be>

<sup>3</sup>The ANS (Advanced Networking Group) research group is part of the Information Engineering Department at the University of Brescia.

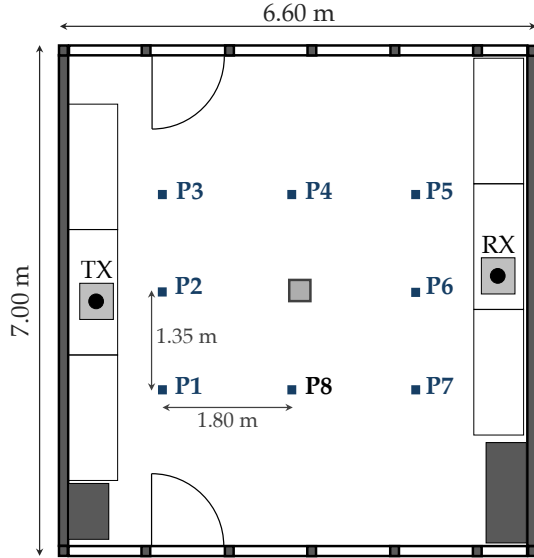


Figure 4: Layout of the experimental setup.

a constant rate of 100 frames per second. Hence, during each data collection session we record a total of 6400 CSI data points over a complete round over the 8 positions, i.e., 800 samples per position. This is repeated twice for every band and Wi-Fi standard under analysis with each collecting session separated by at least 10 minutes. The data collected during the first run is used to train the CNN in the positioning system, and the other dataset is used to test the accuracy of the positioning framework. In this way, training and testing samples do not contain CSI data collected from the same round of experiments, but they are collected in two separate phases ensuring that the accuracy is not biased because the samples for training and testing are collected during a single session. This is inspired by a realistic application scenario in which someone wants to first train the localization framework, and then use it to actually localize a person in a room at a later time. As shown in Fig. 3, the CSI are processed independently one at a time, and each CSI has attached the ground-truth label that is the index of the corresponding position.

## V. RESULTS

As discussed in Section IV, our goal is to evaluate the accuracy of the sensing framework as a function of the Wi-Fi bandwidths. To the best of our knowledge, the question about possible correlations between Wi-Fi bandwidth and sensing accuracy has not been tackled yet, and even recent and accurate surveys ([2], [13]) do not mention studies in this direction, albeit many scholars expect that an increased bandwidth can improve sensing accuracy. Only [14] very recently explored the effect of different channels (namely channel 6 with 20 MHz on the 2.4 GHz band and channel 36 with 80 MHz on the 5 GHz band) found a 6% increase in accuracy using channel 36 when the goal is to count people in a room. However, the authors did not perform experiments to distinguish whether the effect is due to the

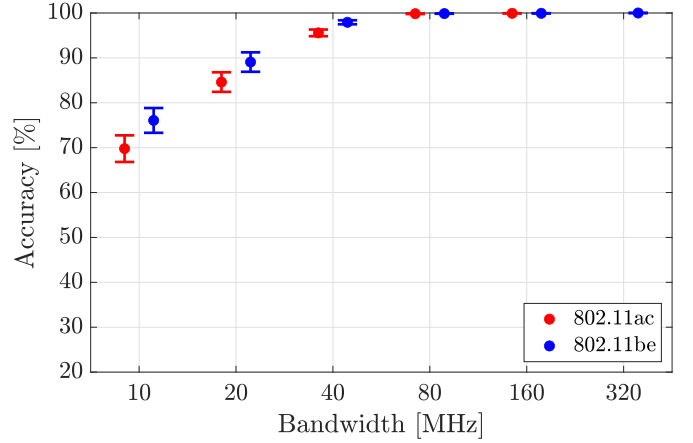


Figure 5: Performance comparison for different Wi-Fi bandwidths using 802.11ac and 802.11be frames. Dots indicate average results over 10 repetitions; vertical bars represent standard deviation. Both training and testing are done collecting 800 CSI per position. Training and testing experiments are separated by at least 10 minutes.

different bandwidth, the different frequency band, or simply less noise and interference in the 5 GHz band.

In our experiments, in addition to the standard Wi-Fi bands, we also consider the 10 MHz band which is used by 802.11p [15], the Wi-Fi version standardized for vehicular communications. This obviously extends our analysis to OFDM systems with an even narrower bandwidth, but also, and more importantly, shed some light on the use of CSI-based sensing in smart mobility spaces and application devised, for instance, to protect Vulnerable Road Users (VRUs). For each band, we collect many CSI data points using both 802.11ac and 802.11be frames, which have sub-carrier spacing of 312.5kHz and 78.125kHz, respectively. The 802.11p standard uses a subcarrier spacing and modulations equivalent to 802.11ac.

Figure 5 shows the experimental results obtained by repeating ten times the training of the CNN for ten epochs, starting each time from a different initial state. The figure reports the average accuracy as a dot and the standard deviation as a vertical bar. When multiple sub-bands are available, average results are shown (e.g., 80-MHz results are averaged across all the sub-bands LL, LH, HL, and HH). Two interesting observations arise from the results reported in Fig. 5. First, larger bands lead to better accuracy of the positioning. Using 320 MHz transmissions leads to the best result, achieving 100% positioning accuracy in our tests. However, using very large channels to get good results is unnecessary, and 80-MHz channels are likely sufficient in the simple scenario we considered. Even 20-MHz transmissions perform quite well, with the average accuracy staying above 80%. Second, the localization with 802.11be frames performs better than that with 802.11ac frames. This is somewhat expected, as 802.11be CSI data has four times the size of the corresponding 802.11ac CSI, and thus can potentially provide more information for the localization task, but the difference is not striking.

Another interesting aspect to explore is the influence of

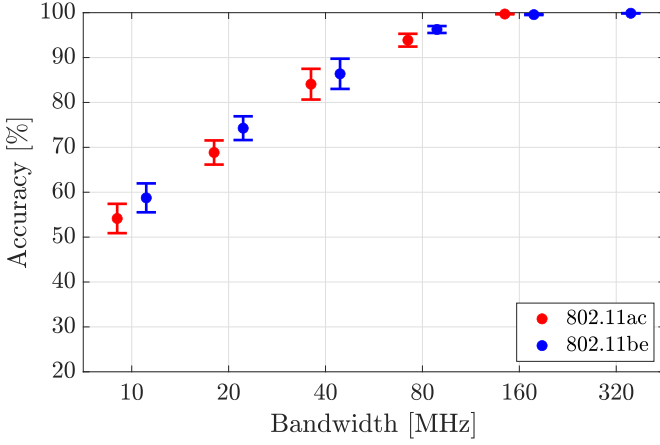
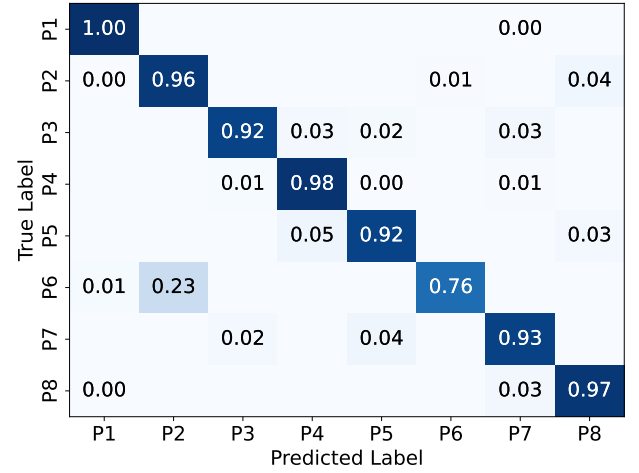


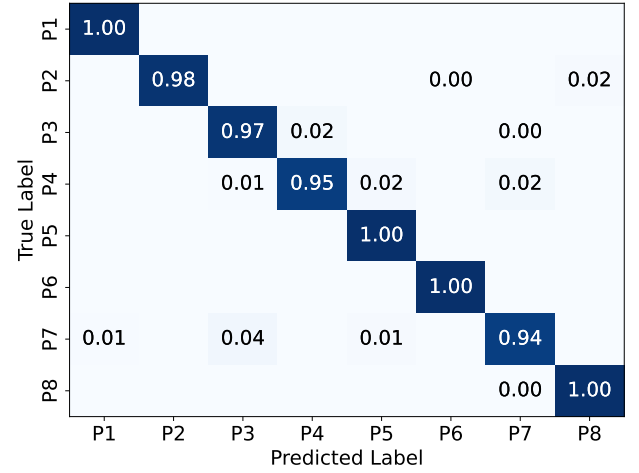
Figure 6: Performance comparison when training the localization model with only 200 samples per position.

different Wi-Fi channels having the same bandwidth but a different position in the spectrum, i.e., to verify whether the *quality* of CSI data for sensing depends in some way on the specific frequencies. Our experimental observations reveal that there is indeed a large variance in the results obtained with 10-MHz sub-channels, where the accuracy can range from a minimum of 38.75% (on channel HLLLH) to a maximum of 96.0% (on channel LLHLH). In general, we observe that the variance decreases as the bandwidth increases. A possible explanation is that the sensing features of the algorithms we use that reveal the position of the target are concentrated in certain sub-bands, and that most probably, these depends on the specific position or the relative layout of sensed positions. This suggests again that CSI sensing on wider Wi-Fi channels can produce better and more “stable” results while using narrower channels can miss some details and quickly lead to overfitting problems during the training phase. This also indicates that the information embedded into a larger-bandwidth signal is not necessarily more, or better, but that on a larger bandwidth there are higher chances to hit the specific frequency that carries the information the localization system is trying to single out.

We continue our analysis by considering how training the model on a limited number of CSI data affects the sensing performance. Thus, we reduce the training dataset to 200 CSI for each target position. The results in Fig. 6 show a reduction in positioning accuracy. This is expected since data-driven models like the CNN used in this work need to be trained on large datasets. The results confirm that the positioning performed with 802.11be frames again has higher accuracy than with 802.11ac frames, and that bandwidth and positioning accuracy are highly correlated. However, using 80-MHz frames is not enough anymore to achieve almost perfect positioning in the new scenario with fewer training samples. Moreover we notice the sensing performance is more affected on Wi-Fi channels with narrower bands. For instance, the accuracy of the model using 40 MHz channels and 802.11ac frames drops from about 95% to 85% on



(a) Training samples collected over 2 seconds.



(b) Training samples collected over 8 seconds.

Figure 7: Confusion matrices obtained by training the positioning model with 40-MHz 802.11ac frames. Only 200 training CSI samples have been used, taken over different intervals of time.

average, while the 10-MHz 802.11ac model’s accuracy drops from 70% to 55%. We recall that these are aggregated results obtained by averaging over all the possible sub-bands and multiple repetitions of the experiments.

We have experimentally verified that the number of OFDM subcarriers directly impacts the sensing accuracy for simple data-driven models. Also, the number of training samples can greatly affect the sensing performance. Another aspect we would like to verify with our experiments is whether it is better to collect CSI data in quick bursts or over longer periods of time. To this end, we consider again only 200 CSI samples per position to train the positioning model, but in one case they are taken in a short period of 2 seconds while in another case they are taken over 8 seconds (i.e., with a sampling frequency of 25 CSI per second). We report in Fig. 7 the classification performance obtained while testing the positioning with 802.11ac frames at 40 MHz. The confusion matrices show that capturing the CSI for longer



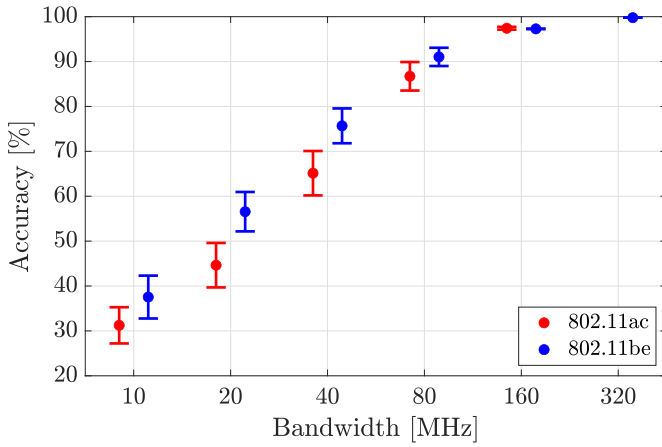


Figure 8: Performance comparison when training the localization model with only 25 CSI per position.

periods of time is better than short bursts. Indeed, taking several CSI measurements in short time periods may miss features that instead are clear on a longer time scale.

Finally, we evaluate what happens to the sensing framework when we reduce the number of training samples even further. Figure 8 shows the positioning accuracy when only 25 CSI for each position are considered to train the CNN. Even in this case, the relation between bandwidth and positioning accuracy is confirmed. The models trained using 160-MHz and 320-MHz frames still perform the best, with accuracy well above 90%. Moreover, it is confirmed that models based on 802.11be frames provide more information for device-free positioning than 802.11ac frames.

## VI. CONCLUSIONS AND FUTURE WORK

After more than ten years of research, CSI-based sensing remains a field of research with many unexplored spaces and corners. This contribution offers a first analysis of the impact of bandwidth on a simple sensing problem concerning device-free positioning. Our preliminary results demonstrate that there seems to be a relation between the performance of the sensing application and the bandwidth of the signals propagating in the environment. Moreover, the IEEE 802.11be frame format (which contains more OFDM subcarriers and even larger 320-MHz channels) can further increase the positioning performance, especially at lower bandwidths.

To run our experiments, we have developed an open-source framework to transmit arbitrary Wi-Fi packets using SDR platforms and measure the corresponding CSI in a controlled setting. Our framework can foster reproducible research on Wi-Fi sensing by simplifying the CSI data collection.

Future work should investigate other sensing algorithms and applications (for example activity and gesture recognition) to confirm whether *i*) bandwidth does influence sensing accuracy in other scenarios or *ii*) some classes of algorithms are more sensitive than others to the bandwidth. We believe that alternative ways to evaluate the time correlation of the CSI can provide additional. In fact, foundational research

on the indoor wireless channels and the causal reasons that enable CSI-based sensing is still needed before these technologies can adequately support future services in wireless networks.

## REFERENCES

- [1] I. Nirmal, A. Khamis, M. Hassan, W. Hu, and X. Zhu, "Deep learning for radio-based human sensing: Recent advances and future directions," *IEEE Comm. Surv. & Tutorials*, vol. 23, no. 2, Feb. 2021.
- [2] C. Chen, G. Zhou, and Y. Lin, "Cross-Domain WiFi Sensing with Channel State Information: A Survey," *ACM Comput. Surv.*, vol. 55, no. 11, Feb. 2023.
- [3] R. Lo Cigno, F. Gringoli, M. Cominelli, and L. Ghiro, "Integrating CSI Sensing in Wireless Networks: Challenges to Privacy and Countermeasures," *IEEE Network*, vol. 36, no. 4, pp. 174–180, Aug. 2022.
- [4] "IEEE Approved Draft Standard for Information technology–Telecommunications and information exchange between systems Local and metropolitan area networks–Specific requirements - Part 11: Wireless LAN Medium Access Control (MAC) and Physical Layer (PHY) Specifications Amendment: Enhancements for Extremely High Throughput (EHT)," *IEEE P802.11be/D7.0*, 2024.
- [5] "IEEE Standard for Information Technology–Telecommunications and Information Exchange between Systems Local and Metropolitan Area Networks–Specific Requirements Part 11: Wireless LAN Medium Access Control (MAC) and Physical Layer (PHY) Specifications Amendment 1: Enhancements for High-Efficiency WLAN," *IEEE Std 802.11ax-2021 (Amendment to IEEE Std 802.11-2020)*, 2021.
- [6] Z. Jiang, T. H. Luan, X. Ren, *et al.*, "Eliminating the barriers: Demystifying wi-fi baseband design and introducing the picoscenes wi-fi sensing platform," *IEEE Internet of Things Jou.*, vol. 9, no. 6, pp. 4476–4496, 2022.
- [7] F. Gringoli, M. Cominelli, A. Blanco, and J. Widmer, "Ax-csi: Enabling csi extraction on commercial 802.11ax wi-fi platforms," in *15th ACM Wrks on Wireless Network Testbeds, Experimental Evaluation & Characterization (WiNTECH)*, ser. WiNTECH '21, Association for Computing Machinery, 2021, pp. 46–53.
- [8] D. Halperin, W. Hu, A. Sheth, and D. Wetherall, "Tool release: gathering 802.11n traces with channel state information," *SIGCOMM Comput. Commun. Rev.*, vol. 41, no. 1, p. 53, Jan. 2011.
- [9] J. Wan, T. Jiang, X. Zhou, and D. Huang, "Wi-locind: Location-independent respiration sensing based on wifi csi," in *2024 IEEE Wireless Communications and Networking Conference (WCNC)*, 2024.
- [10] C. Cai, L. Deng, M. Zheng, and S. Li, "Pilo: Passive indoor localization based on convolutional neural networks," in *2018 Ubiquitous Positioning, Indoor Navigation and Location-Based Services (UPINLBS)*, 2018.
- [11] M. Cominelli, F. Kosterhon, F. Gringoli, R. Lo Cigno, and A. Asadi, "IEEE 802.11 CSI randomization to preserve location privacy: An empirical evaluation in different scenarios," *Elsevier Computer Networks*, vol. 191, no. 22, May 2021.
- [12] M. Cominelli, F. Gringoli, and R. Lo Cigno, "AntiSense: Standard-compliant CSI obfuscation against unauthorized Wi-Fi sensing," *Elsevier Computer Communications*, vol. 185, pp. 92–103, Mar. 2022.
- [13] Ma, Y. and Zhou, G. and S. Wang, S., "WiFi Sensing with Channel State Information: A Survey," *ACM Comp. Surv.*, vol. 52, no. 46, pp. 1–36, Jun. 2019.
- [14] H. Guan, A. Sharma, D. Mishra, and A. Seneviratne, "Experimental Accuracy Comparison for 2.4GHz and 5GHz WiFi Sensing Systems," in *IEEE ICC 2023, Rome, Italy, May 2023*, pp. 4755–4760.
- [15] "IEEE Standard for Information technology– Local and metropolitan area networks– Specific requirements– Part 11: Wireless LAN Medium Access Control (MAC) and Physical Layer (PHY) Specifications Amendment 6: Wireless Access in Vehicular Environments," *IEEE Std 802.11p-2010*, 2010.